www.elsevier.com/locate/talanta

Automated flow fluorescent noncompetitive immunoassay for measurement of human plasma levels of monoclonal antibodies used for immunotherapy of cancers with KinExA^{TM} 3200 biosensor

Haitham AlRabiah, Mohammed A. Hamidaddin, Ibrahim A. Darwish

PII: S0039-9140(18)30924-X
DOI: https://doi.org/10.1016/j.talanta.2018.09.014
Reference: TAL19028

To appear in: *Talanta*

Received date: 24 May 2018
Revised date: 5 September 2018
Accepted date: 5 September 2018

Cite this article as: Haitham AlRabiah, Mohammed A. Hamidaddin and Ibrahim A. Darwish, Automated flow fluorescent noncompetitive immunoassay for measurement of human plasma levels of monoclonal antibodies used for immunotherapy of cancers with KinExA^{TM} 3200 biosensor, *Talanta,* https://doi.org/10.1016/j.talanta.2018.09.014

Automated flow fluorescent noncompetitive immunoassay for measurement of human plasma levels of monoclonal antibodies used for immunotherapy of cancers with KinExA™ 3200 biosensor

Haitham AlRabiah[1], Mohammed A. Hamidaddin[1,2], Ibrahim A. Darwish[1]*

[1]Department of Pharmaceutical Chemistry, College of Pharmacy, King Saud University, P.O. Box 2457, Riyadh 11451, Saudi Arabia.

[2]Department of Medicinal and Analytical Chemistry, Faculty of Pharmacy, Sana'a University, Sana'a, Yemen.

*Corresponding Author: Ibrahim A. Darwish, Prof. Fax: +966-114676220, Tel: +966-114677348, E-mail: idarwish@ksu.edu.sa

ABSTRACT

This study describes, for the first time, the development of an automated sensitive flow fluorescent noncompetitive immunoassay based on kinetic-exclusion analysis (KinExA) for the quantitative determination of human plasma levels of monoclonal antibodies (mAbs) used for cancer immunotherapy. The assay was adapted on KinExA™ 3200 biosensor and optimized and validated for bevacizumab (BEV) and cetuximab (CET), as representative examples of the mAbs, using their specific antigens. These antigens were the human vascular endothelial growth factor (VEGF) and epidermal growth factor receptor (EGFR) for BEV and CET, respectively. The limits of detection were 1.28 and 52.64 ng mL^{-1} for BEV and CET, respectively. The accuracy of the assay was demonstrated with analytical recovery of analytes from spiked plasma at 96.2 – 104.3 and 96.8 – 105.3% for of BEV and CET, respectively. The precision of the assay was satisfactory as shown by relative standard deviation (RSD) at 2.2 – 5.7 and 2.5 – 6.1% for

assay of BEV and CET, respectively. The high sensitivity of the assay allowed the use of very small volumes (~ 1 µL) of plasma sample for analysis. Automated analysis by the proposed KinExA-based assay facilitates the processing of large numbers of mAbs-containing specimens in studies of pharmacokinetics (PK), pharmacodynamics (PD), and therapeutic drug monitoring (TDM) of therapeutic mAbs. The proposed assay can be used to overcome the problems encountered in the existing conventional immunoassays for mAbs.

Graphical Abstract

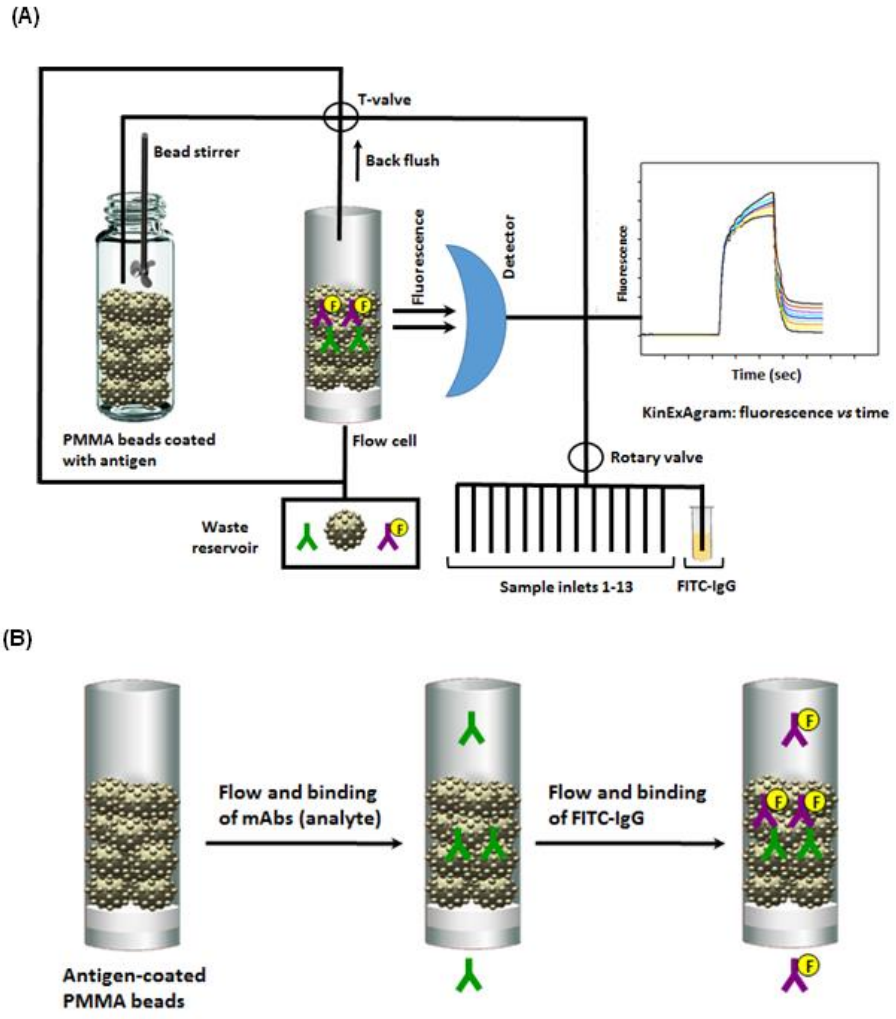

Keywords: Immunotherapy; Monoclonal antibodies; Bevacizumab; Cetuximab; Immunoassay; KinExA.

1. Introduction

Immunotherapy is a novel promising intervention, attracting much attention in cancer therapy [1]. Drugs used for immunotherapy of cancer are human (or humanized) monoclonal antibodies (mAbs) that can assist the body's immune system in recognizing and attacking cancer cells [2–6]. Compared to chemotherapeutic small-molecule drugs (e.g. tyrosine kinase inhibitors), therapeutic mAbs are safer and provide better pharmacokinetic (PK) and pharmacodynamic (PD) features. Therefore, developing therapeutic mAbs has become one of the fastest growing areas of the pharmaceutical/biotechnological industries [7–10]. The US Food and Drug Administration (FDA) has to date approved many mAbs for the immunotherapy of different types of cancers [11]. The effects of most therapeutic mAbs depend on their concentrations and their pharmacokinetic patterns which are not linear. This is partly attributed to the neonatal Fc receptor which functions in catabolism of mAbs before reaching to the blood and binding to their targets [12–15]. This necessitates a closer monitoring of their plasma levels during therapy.

Liquid chromatography coupled with tandem mass spectrometric detection (LC-MS/MS) is a potential technique for measurement of therapeutic mAbs in biological specimens. However, there are several challenges associated with the development of LC-MS/MS methods, such as the complexity of sample matrices, time-consuming trypsin digestion, multi-step laborious purification steps, and the absence of an efficient strategy to develop an optimal LC-MS/MS method. In addition, its high cost and instrumentation complexity limit its routine application in clinical laboratories [16]. Despite the development of several methods for improving and speeding up the procedures of trypsin digestion [17,18] and sample purification [19], complicated preparation procedures are still challenging, including, denaturation, reduction and alkylation before digestion [20]. In addition, most of these methods still suffering from major drawbacks, such as discrepancies in chromatography peaks [20], unsatisfactory precision and sensitivity along with the time consuming and laborious nature of the analysis protocol [21,22].

Principally, immunoassays are the most recommended methods for quantitation of macromolecules, such as therapeutic mAbs in biological fluids [23]. Different enzyme-linked immunosorbent assays (ELISAs) have been described for the determination of therapeutic mAbs to support pharmaceutical quality control, PK, PD, and TDM [24–26]. However, most of these assays involve the use of an assay plate coated with commercial anti-idiotype antibodies to capture therapeutic mAbs from their specimen solutions. This approach may cause false positive

results due to non-specific capturing of similar human IgG antibodies in the specimens [25]. In addition, inaccurate results were also observed with values of coefficients of variation of >20% [26]. To overcome these drawbacks, we describe the development of an automated flow fluorescent noncompetitive immunoassay with KinExA™ 3200 system for quantitative determination of therapeutic mAbs in human plasma samples.

KinExA systems represent the most important technological progress with exceptional unique features, in the field of biomedical analysis [27–30]. These systems offer a direct interface of an immunochemical reaction with a fluorescent signal transducer, and the strength of the generated signals is related to the analyte concentration. KinExA systems are used primarily in determination of true-liquid phase equilibrium association/dissociation constants of antibodies [31-33]. In previous studies, Darwish *et al*. [34-37] explored the use of KinExA systems for the quantitative analysis of analytes of diverse nature. These KinExA-based assays offered several advantages over conventional immunoassays (e.g. ELISA), such as eliminating the negative effect of the immobilization of anti-analyte antibodies onto assay plates on the analytical results, bypassing the mass transport limitations encountered with ELISA, and providing higher sensitivities and better convenience. Although KinExA systems were previously used for studying the binding affinities of the therapeutic mAbs; however, KinExA-based assays have not yet been described for quantitative analysis in plasma samples.

Therefore, the present study describes, for the first time, the development of KinExA-based automated sensitive fluorescent noncompetitive immunoassay for the measurement of plasma levels of mAbs.

2. Experimental

2.1. Instruments

KinExA™ 3200 biosensor (Sapidyne Instruments Inc., Boise, ID, USA). Incubator (Model MINI/18, Genlab Ltd. Widnes, UK). Nutating mixer (Taitec, Saitama-ken, Japan). Microprocessor Laboratory pH meter, BT-500 (Boeco, Hamburg, Germany). Milli-Q water purification system (Millipore Ltd., Bedford, USA).

2.2. Materials

BEV and CET were purchased from BOC Sciences (NJ, USA). Recombinant human vascular endothelial growth factor VEGF-165 protein was purchased from R&D Systems (Lille, France). Recombinant human epidermal growth factor receptor (EGFR) was purchased from Sigma-Aldrich (St. Louise, MO, USA). PMMA beads (140-170 mesh, 98 µm) were purchased from Sapidyne Instruments Inc. (Boise, ID, USA). Bovine serum albumin (BSA) and FITC-IgG conjugate were obtained from Sigma-Aldrich LLC (CA, USA). Human plasma was obtained from Blood Bank of King Saud University Medical City (Riyadh, Saudi Arabia). All other chemicals used throughout the work were of analytical grade.

2.3. Techniques and procedures

2.3.1. Coating of VEGF and EGFR onto PMMA beads

PMMA bead vials containing 200 mg (dry weight) of beads were coated separately with each of VEGF and EGFR. The coating solution comprised of 1 mL of phosphate buffered saline (PBS: 10 mM sodium phosphate, 137 mM NaCl and 3 mM KCl, pH 7.4) containing 50 µg/mL of VEGF or EGFR. Bead vials containing the coating solution were kept on the nutating mixer for 2 h at room temperature (25 ± 2 °C). The bead vials were then taken off from the mixer and the beads were allowed to settle down at the bottom of the vials. The supernatant was removed and replaced with 1 mL of BSA solution (1%, w/v, in PBS). The bead vials were transferred again to the nutating mixer for a further a period of 1 h to block the remaining protein-binding sites on the coated beads. Later, the coated beads were removed and stored at 4 °C in refrigerator and were stable for a period of 5 days after coating.

2.3.2. Analysis on KinExA™ 320 instrument

The KinExA™ 320 instrument has 14 sampling lines of which 12 lines were separately placed into a sample tube containing BEV or CET (50 and 100 µg mL^{-1} mL in PBS containing 0.1%, w/v BSA, respectively), calibrator solutions or spiked plasma samples. The 13^{th} line was placed into a tube containing blank (zero concentration of BEV or CET), and the 14^{th} line was placed into a tube containing FITC-IgG solution. The beads coated with VEGF or EGFR (for assay of BEV or CET, respectively) were loaded into the bead reservoir of the KinExA™ 3200 instrument and further diluted with 30 mL of PBS. The bead reservoir contains a stirrer which

ensures even distribution of beads during each bead charge to form a microcolumn of beads. The beads were charged twice at the start of the experiment to ensure appropriate bead height during the experiment. The bead height can be monitored manually with the help of a camera installed inside the flow cell. The column height is managed by altering either the flow time or the flow volume from the bead reservoir. A flow volume of 583 µL at a flow rate of 1 mL min^{-1} provided the desired height of the bead column. The bead columns produced under these conditions were identical and reproducible. The instrument analyzed the samples starting from inlet-1 to inlet-13. Each aspirated sample (500 µL) at flow rate of 0.25 mL min^{-1} was passed for 120 sec over the freshly generated bead column. A buffer wash using 125 µL of PBS for 30 sec followed sample aspiration to remove free excess unbound BEV or CET molecules from the bead column. FITC-IgG solution (500 µL of 0.2 and 2 µg mL^{-1} in PBS containing 0.1%, w/v BSA for assay of BEV and CET, respectively) was aspirated and passed over the bead column. A buffer wash using 1.5 mL of PBS for 90 sec at a flow rate of 1 mL min^{-1} was performed to remove any unbound FITC-IgG. The camera used for monitoring the flow/ observation cell assisted with this procedure. The data were collected by KinExA Pro 20.0.1.26 software provided with the KinExA instrument, and transformed using linear curve fitting to generate the calibration curve. The calibration curve was used to measure the plasma concentrations of the mAbs.

3. Results and discussion

3.1. Strategy for selection of the target analytes and assay design

BEV and CET are mAbs frequently prescribed for immunotherapy of various types of cancer (colon, renal, ovarian, certain types of lung cancers and glioblastoma) via targeting cancer cell growth factor receptors [4,5]. BEV is a recombinant humanized mAb that targets VEGF [38], leading to inhibition of its biologic activities and a reduction in microvascular growth of tumor blood vessels [39,40]. CET is a chimeric (mouse/human) mAb that targets EGFR [41]. It blocks the binding of ligands to EGFR, thereby inhibiting receptor phosphorylation and downstream events [42]. The patent of BEV expired in April 2017 [43], and expectedly BEV biosimilars and/or biobetters will be produced by many pharmaceutical companies. Similarly, CET patent expired in February 2016, and some of its biosimilars have been recently produced [44]. Accordingly, there will be increasing demand for appropriate assays for the bioanalysis of BEV

and CET in their bioequivalence studies and therapeutic monitoring during therapy. These reasons were behind our interest in selecting BEV and CET as representative examples of therapeutic mAbs to be the target analytes in the development of the assay described herein using their commercially available specific antigens; VEGF and EGFR for BEV and CET, respectively.

For selecting the assay format, many different immunoassay formats could possibly be adapted [45,46]; however, we selected noncompetitive binding format because it usually offers high accuracy and limited variance at low analyte concentrations. Because of the aforementioned advantages of KinExA-based assays, we decided to interface noncompetitive binding of BEV and CET with their antigens with the KinExA^{TM} 3200 system for signal transducer. Since BEV and CET mAb are of IgG subtype, anti-human IgG antibody conjugated to FITC was used to assess the binding reaction of BEV and CET to VEGF and EGFR, respectively. FITC was considered as a fluorescence-generating label because of its documented high fluorescence quantum yield that enables development of highly sensitive assays, in addition to its good photostability and a low temperature coefficient [46].

3.2. Description of KinExA assay

Details of the KinExA^{TM} 3200 system setup and working are described in its operation manual and in previous reports [47-53]. Figure 1 provides a schematic presentation for the operation of the KinExA system for conducting the assay described herein. Samples containing varying concentrations of each of BEV and CET were drawn onto the bead microcolumn containing PMMA beads coated with antigens (VEGF and EGFR for assay of BEV and CET, respectively) for a very brief period of time. The BEV and CET molecules with free binding sites interact with their corresponding immobilized antigens coated onto the beads. Any remaining BEV and CET molecules present in the bead column were removed by an immediate buffer wash. FITC-IgG was then aspirated over the bead column on which BEV and CET molecules have been captured by their antigens coated onto the PMMA beads. Accordingly, the amount of FITC-IgG retained on the beads is related quantitatively with the amount of BEV or CET captured on the beads. After this, a wash step was performed to remove any excess unbound FITC-IgG present on the bead column, and the fluorescence intensity was measured by the photodiode provided in the KinExA^{TM} 3200 system. The real trend-line fluorescence

responses (KinExAgram) generated in the assays of BEV and CET are given in Fig. 2. The monitored fluorescence signals were those at the end of the KinExAgram, after the unbound FITC-labeled antibody has been washed from the bead column.

3.3. Optimization of KinExA signals

For analysis on KinExA, two signals should be determined; these signals were the net and nonspecific signals. The net signal was generated at a definite known concentration of the analyte (BEV or CET) that bound to the antigen-coated PMMA beads. The nonspecific signal was the signal generated due to nonspecific binding of the FITC-IgG to the antigen-coated beads at zero concentration of the analyte (PBS buffer). For analysis, the nonspecific signal was subtracted from the nonspecific signal. Therefore, it is worth mentioning that the reproducibility of the results depends on low background noise due to the nonspecific signals attributed to insufficient washing of the bead column as reagents stick to the column walls. In order to reduce background noise, the instrument is thoroughly rinsed using fast- and overnight-wash.

3.4. Optimization of assay conditions

3.4.1. Selection of VEGF and EGFR concentrations for coating onto the PMMA beads

Because the assay involved noncompetitive binding of BEV and CET to their corresponding antigens (VEGF and EGFR, respectively coated onto PMMA beads), the concentrations of these antigens should be in excess to be able to capture all the possible BEV and CET molecules in the samples. Therefore, high concentrations of BEV and CET (20 and 500 ng mL^{-1}, respectively) were used to establish the optimum concentrations of their antigens required for coating PMMA beads. Varying concentrations of each of VEGF and EGFR (6.25−100 μg mL^{-1}) were coated the beads and used in the assay. The signals (after subtraction of the background's signals) were plotted as a function of antigen concentration. It was found that the saturating concentrations of VEGF and EGFR were 25 μg mL^{-1} for both BEV and CET (Fig. 3). However, to ensure excess of VEGF and EGFR is used, a higher concentration (50 μg mL^{-1}) of both antigens was used in all the subsequent experiments.

3.4.2. Selection of FITC-IgG concentrations

In the KinExA-based analysis, it is most important to consider that the net signal (signal generated due to antigen-antibody binding reaction) should be above zero and reasonably reproducible. In addition, a reasonable goal is to obtain a net signal in the range of 0.5 − 1.5 millivolts [47]. In order to select the most appropriate concentration of the FITC-IgG required for attaining the ideal signal, varying concentrations of FITC-IgG (25−500 ng mL^{-1}) for BEV assay and (0.25 – 8.00 µg mL^{-1}) for CET assay were used, and the signals were generated using fixed concentrations of BEV and CET (20 and 500 ng mL^{-1}, respectively). The signals (after subtraction of the background's signals) were plotted as a function of FITC-IgG concentration. It was found that the net signals increase as the FITC-IgG concentration increases, and the reasonable constant net signals were obtained when the FITC-IgG concentrations were in the range of 100 − 200 ng mL^{-1} and 1 – 3 µg mL^{-1} for BEV and CET, respectively (Fig. 4). Beyond these concentrations, the signals decreased. FITC-IgG concentrations of 200 ng/mL and 2 µg mL^{-1} were ultimately used for assay of BEV and CET, respectively.

The established optimum conditions, in addition to other optimized instrumental conditions for running the KinExA system were used in the present assay. A summary for these conditions is provided in Table 1.

3.4.3. Analysis of mAbs by KinExA-based assay

The instrument starts to record the response as soon as the bead column is formed and keeps on recording the response even during the buffer wash (to remove unbound samples). The instrument responses as a function of time (KinExAgrams) for running various concentrations of BEV and CET are shown in Fig. 2. The background signal recording lasts from 0 to 165 sec and is generated while BEV or CET in the samples are exposed to the bead-packed microcolumn and captured by their corresponding antigens coated onto the beads, and eventually, washed out of the bead column. The next step is flow of FITC-IgG over the bead column and its capture by the BEV and CET bound to antigens-coated beads. This process occurs at 166 – 280 sec followed by a washing step at 281 – 385 sec to remove any excess FITC-IgG molecules trapped on the bead column. The sample in inlets 1 − 12 contained varying concentrations of either BEV (1.25 − 20 ng/mL) or CET (50 − 500 ng mL^{-1}) and the sample inlet-13 did not contained any free BEV or

CET (0 concentrations, corresponding to the lowest curve in the KiExAgrams). The generated signals are represented as square waves corresponding to the fluorescence of FITC-IgG during transient passage over the beads in the observation cell of the KinExA system.

3.5. Validation of the assay

3.5.1. Calibration curve, assay precision and sensitivity

Under the established optimum conditions of the proposed KinExA assay, calibration curves for the determination of BEV and CET were constructed by plotting the net fluorescence signals (after subtraction of the background's signals) were plotted as a function of the corresponding concentrations (Fig. 5). The regression analysis of the data (Table 2) showed high determination coefficients (r^2), on the linear curve fit; the regression equations were:

For BEV: $F = 0.1782 + 0.0693C$ ($r^2 = 0.994$)

For CET: $F = 0.0163 + 0.0011C$ ($r^2 = 0.987$)

Where; F is the net fluorescence signal (millivolts); C is the concentration of BEV or CET in ng mL^{-1}.

The linear dynamic ranges of the assays were 1.25 – 20 and 50 – 500 ng mL^{-1} for BEV and CET, respectively. The limits of detection (LOD) and limits of quantification (LOQ) of the assays were determined as per the guidelines of the International Conference of Harmonization (ICH) for validation of analytical procedures [54]. The following formula was used: LOD or LOQ = $\times SD_a/b$; where: $\times$ = 3.3 for LOD and 10 for LOQ, SD_a is the standard deviation of the intercept, and b is the slope. For BEV, the LOD and LOQ were found to be 1.28 and 3.89 ng mL^{-1}, respectively. For CET, the LOD and LOQ were found to be 52.64 and 159.52 ng mL^{-1}, respectively. This high sensitivity of the present KinExA assay enables the determination of BEV and CET in plasma samples as the reported average maximum concentrations were 323 and 228.9 µg mL^{-1} for BEV [55] and CET [42], respectively.

The precision profiles obtained from the results of calibration samples, assayed in duplicates, are shown in Fig. 5. The relative standard deviation (RSD) values were less than 10% throughout the entire working range of the assays.

3.5.2. Effect of plasma matrix

The proposed assay was designed for quantitation of mAbs in plasma samples; therefore, it was necessary to study the effect of plasma matrix on the assay accuracy to avoid false positive or negative effects in the application of assay to plasma samples. In this study, drug-free plasma samples were serially diluted in PBS and each dilution was separately spiked with the reported therapeutic plasma levels of BEV and CET (323 and 229 μg mL^{-1}, respectively) and the samples were diluted to attain the BEV and CET in the working range of their assays (15 and 400 ng mL^{-1} of BEV and CET, respectively). The spiked-diluted samples were then analyzed by the KinExA assay as a routine procedure; KinExAgrams are provided in Fig. 6 (panels A and B). The matrix effects were assessed using the recovery levels calculated with the calibration curves generated with 1× PBS. The recoveries as a function of plasma dilutions are shown in Fig. 6 (panel C). It is obvious that the recovery percentage values increase with the plasma dilution, and then leveled off to ~100% when the plasma dilution was 32- and 64-fold for BEV and CET, respectively (Fig. 6C). These data indicated that the assay could be suitable for direct application on plasma samples diluted at least 32-fold with PBS before their analysis by the KinExA system.

It is worth mentioning that the reported therapeutic concentrations of BEV in plasma are in the range of 100 – 323 μg mL^{-1} [55] and the maximum plasma concentration of CET is 229 μg mL^{-1} [42]. Therefore, plasma samples containing these high concentrations (in μg-scale) should be diluted with PBS at least 20,000- and 1,400-fold (for BEV and CET, respectively) to attain the concentrations of BEV and CET in the working range of the assay (LOQ was 3.89 and 159.5 ng mL^{-1} for BEV and CET, respectively). These data proved the applicability of the assay to the analysis of mAbs in plasma samples without any negative matrix effect on the assay results. In addition, the high dilution of plasma samples required prior to the analysis allowed the use of very small plasma samples from patients; 1 μL of plasma was adequate for dilution with PBS to 1 mL solution for analysis by the KinExA system. The use of very small plasma samples made the assay convenient when applied in clinical laboratories.

3.5.3. Precision and accuracy

The intra-assay precision of the KinExA assay was determined at varying concentration levels of BEV and CET (2–16 and 100–400 ng mL^{-1}, respectively) by analyzing 3 replicates of each sample as a batch in a single assay run. The inter-assay precision was determined by

analyzing the same samples as duplicates in three consecutive separate runs. According to the recommendations of immunoassay validation [56], the assays gave satisfactory precisions; the RSD did not exceed 6.1% (Table 3). The high precision of the proposed KinExA-based assay was attributed mainly to the use of high excess concentration of capturing antigens-coated beads with high surface area. This condition made the assay precision dependent only on the concentrations of the mAb and FITC-IgG, which were dispended automatically with high precision by the KinExA instrument.

The accuracy of the proposed KinExA-based assay was evaluated by determination of the recovery of varying concentrations (2 – 16 and 100 – 400 ng mL^{-1} for BEV and CET, respectively) spiked in plasma samples and diluted with PBS solution. The obtained recovery values for BEV were 96.2 ± 4.8 – 104.3 ± 4.2%, and those for CET were 96.8 ± 5.3 – 105.3 ± 5.2% (Table 4). These recovery values, as per the recommendations of immunoassay validation [56], indicated the accuracy of the assay for BEV and CET.

3.5.4. Comparison of the proposed KinExA-based assay with ELISA

Different forms of ELISAs with varying sensitivities have been developed for determination of BEV [24,57,58] and CET [25,26,59,60] in different sample matrices. The LOD values of these assays were in the range of 0.05 – 3 ng mL^{-1} and 0.01 – 0.31 μg mL^{-1} for BEV and CET, respectively. The variation in LOD values was attributed to the assay formats and enzyme labels/ enzyme substrates involved in the assay development. The LOD values of the proposed KinExA-based assay were 1.28 and 52.64 ng mL^{-1} for BEV and CET, respectively. These values indicated that the sensitivity of the KinExA-based assay for BEV is an intermediate among its existing ELISAs. However, the KinExA-based assay for CET is higher than its existing ELISAs.

In order to make a realistic comparison between the present KinExA-based assays and ELISA formats, we developed ELISA for BEV [61] and CET [62] in our laboratory using identical reagents, and compared the sensitivities of both assay formats. The LOD values for our ELISAs were 1.01 and 1.5 ng mL^{-1} for BEV and CET, respectively, compared with 1.28 and 52.64 ng mL^{-1} for KinExA-based assays, respectively. Although, the KinExA-based assay for CET was less sensitive than its ELISA; however, the sensitivities of KinExA assays were adequate for bioanalysis of both BEV and CET in their clinical samples.

4. Conclusions

The present study described, for the first time, the development and validation of an automated flow fluorescent immunoassay for the measurement of human plasma levels of mAbs used for immunotherapy of cancers. The assay was developed using BEV and CET, as representative examples of mAbs. The assay employed noncompetitive binding reaction interface on a KinExA^{TM} 3200 system for automated analysis of samples by measurement of fluorescence signals directly onto bead column inside the flow cell of the KinExA system. The assay was able to quantify BEV and CET at concentrations as low as 3.89 and 159.52 ng mL^{-1}, respectively. The high sensitivity of the assay allowed use of very small volumes (~ 1 µL) of plasma samples for analysis. The KinExA assay provides several advantages over the existing conventional ELISA technique for mAbs such as reduction in mass transport limitation and mobility effects. The ability of KinExA to run samples automatically makes the assay powerful tool for high throughput analysis of plasma samples in studying PK, PD, TDM of immunotherapy, and evaluating the biological equivalencies in discovery of biosimilars or biobetters. Although the assay was developed and validated for BEV and CET, it can also be adapted to the analysis of any mAb as long as a specific antigen is available.

Acknowledgements

The authors would like to extend their appreciation to the Deanship of Scientific Research at King Saud University for its funding of this research through the research group No. RGP-225.

Conflict of interest

No conflict of interest is declared.

References

[1] D.F. Heigener, M. Reck, New approaches in immunotherapy, in: Peters S., Besse B. (Eds.), New Therapeutic Strategies in Lung Cancers, Springer International Publishing, Switzerland, 2015.

[2] L.M. Weiner, R. Surana, S. Wang, Monoclonal antibodies: versatile platforms for cancer immunotherapy, Nat. Rev. Immunol. 10 (2010) 317–327.

[3] J.M. Clarke, H.I. Hurwitz, Targeted inhibition of VEGF receptor 2: an update on ramucirumab, Expert Opin. Biol. Ther. 13 (2013) 1187–1196.

[4] R. Pirker, J.R. Pereira, A. Szczesna, J. von Pawel, M. Krzakowski, R. Ramlau, I. Vynnychenko, K. Park, C.T. Yu, V. Ganul, J.K. Roh, E. Bajetta, K. O'Byrne, F. de Marinis, W. Eberhardt, T. Goddemeier, M. Emig, U. Gatzemeier; FLEX Study Team, Cetuximab plus chemotherapy in patients with advanced non-small-cell lung cancer (FLEX): an open-label randomised phase III trial, The Lancet 373 (2009) 1525–1531.

[5] T.E. Stinchcombe, M.A. Socinski, Bevacizumab in the treatment of non-small-cell lung cancer, Oncogene 26 (2007) 3691–3698.

[6] A. Karlitepe, O. Ozalp, C.Biray, New approaches for cancer immunotherapy, Tumour Biol. 36 (2015) 4075–4078.

[7] E.D. Lobo, R.J. Hansen, J.P. Balthasar, Antibody pharmacokinetics and pharmacodynamics, J. Pharm. Sci. 93 (2004) 2645–2668.

[8] L. Guilleminault, E. Lemarié, N. Heuzé-Vourc'h, Monoclonal antibodies: an emerging class of therapeutics in non small cell lung cancer, J. Cancer Ther. 3 (2012) 1170–1190.

[9] F.R. Brennan, L.D. Morton, S. Spindeldreher, A. Ki-essling, R. Allenspach, A. Hey, P.Y. Muller, W. Frings, J. Sims, Safety and immunotoxicity assessment of immunomodulatory monoclonal antibodies, MAbs 2 (2010) 233–255.

[10] T.T. Hansel, H. Kropshofer, T. Singer, J.A. Mitchell, A.J.T. George, The safety and side effects of monoclonal antibodies, Nat. Rev. Drug Discov. 9 (2010) 325–338.

[11] C. Helissey, C. Vicier, S. Champiat, The development of immunotherapy in older adults: new treatments, new toxicities?, J. Geriatr. Oncol. 7(2016) 325–333.

[12] W. Wang, E.Q. Wang, J.P. Balthasar, Monoclonal antibody pharmacokinetics and pharmacodynamics, Clin. Pharmacol. Ther. 84 (2008 548–558.

[13] T. Suzuki, A. Ishii-Watabe, M. Tada, T. Kobayashi, T. Kanayasu-Toyoda, T. Kawanishi, T. Yamaguchi, Importance of neonatal FcR in regulating the serum half-life of therapeutic proteins containing the Fc domain of human IgG1: a comparative study of the affinity of monoclonal antibodies and Fc fusion proteins to human neonatal FcR, J. Immunol. 184 (2010) 1968–1976.

[14] C.M. Ng, E. Stefanich, B.S. Anand, P.J. Fielder, L. Vaickus, Pharmacokinetics/ pharmacodynamics of nondepleting anti-CD4 monoclonal antibody (TRX1) in healthy human volunteers, Pharm. Res. 23 (2006) 95–103.

[15] N. Hayashi, Y. Tsukamoto, W.M. Sallas, P.J. Lowe, A mechanism-based binding model for the population pharmacokinetics and pharmacodynamics of omalizumab, Br. J. Clin. Pharmacol. 63 (2007) 548–561.

[16] X. Duan, L. Abuqayyas, L. Dai, J.P. Balthasar, J. Qu, High-throughput method development for sensitive, accurate, and reproducible quantification of therapeutic monoclonal antibodies in tissues using orthogonal array optimization and nano liquid chromatography/selected reaction monitoring mass spectrometry, Anal. Chem. 84 (2012) 4373–4382.

[17] K.J. Bronsema, R. Bischoff, W.W.M. Pim Pijnappel, A.T. van der Ploeg, N.C. van de Merbel, Absolute quantification of the total and antidrug antibody-bound concentrations of recombinant human α-glucosidase in human plasma using protein G extraction and LC-MS/MS, Anal. Chem. 87 (2015) 4394–4401.

[18] B. An, M. Zhang, R.W. Johnson, J. Qu, Surfactant-aided precipitation/on-pellet-digestion (sod) procedure provides robust and rapid sample preparation for reproducible, accurate and sensitive LC/MS quantification of therapeutic protein in plasma and tissues, Anal. Chem. 87 (2015) 4023–4029.

[19] Y. Shen, G. Zhang, J. Yang, Y. Qiu, T. McCauley, L. Pan, J. Wu, Online 2D-LC-MS/MS assay to quantify therapeutic protein in human serum in the presence of pre-existing antidrug antibodies, Anal. Chem. 87 (2015) 8555–8563.

[20] C. Wegler, F.Z. Gaugaz, T.B. Andersson, J.R. Wiśniewski et al., Variability in mass spectrometry-based quantification of clinically relevant drug transporters and drug metabolizing enzymes, Mol. Pharm. 14 (2017) 3142–3151.

[21] C.W. Damen, E.J.Derissen, J.H. Schellens, H.Rosing, J.H. Beijnen, The bioanalysis of the monoclonal antibody trastuzumab by high-performance liquid chromatography with fluorescence detection after immuno-affinity purification from human serum, J. Pharm. Biomed. Anal. 50 (2009) 861–866.

[22] K. Todoroki, T. Nakano, Y. Eda, K. Ohyama, H. Hayashi, D. Tsuji, J.Z. Min, K. Inoue, N. Iwamoto, A. Kawakami, Y. Ueki, K. Itoh, T. Toyo'oka, Bioanalysis of bevacizumab and infliximab by high-temperature reversed-phase liquid chromatography with fluorescence detection after immunoaffinity magnetic purification, Anal. Chim. Acta. 916 (2016) 112–119.

[23] I.A. Darwish, Immunoassay methods and their applications in pharmaceutical analysis: basic methodology and recent advances, Intl. J. Biomed. Sci. 2 (2006) 217–235.

[24] I. Suárez, A. Salmerón-García, J. Cabeza, L.F. Capitán-Vallvey, N. Navas, Development and use of specific ELISA methods for quantifying the biological activity of bevacizumab, cetuximab and trastuzumab in stability studies, J. Chromatogr. B Analyt. Technol. Biomed. Life Sci. 1032 (2016) 155–164.

[25] Somru BioScience Inc, Cetuximab (Erbitux®) PK ELISA, Catalog SBA-100-007-015, 2017. http://www.deltaclon.com/pdf/somru/SBA-100-007-015.pdf.

[26] N. Cézé, D. Ternant, F. Piller, D. Degenne, N. Azzopardi, E. Dorval, H. Watier, T. Lecomte, G. Paintaud, An enzyme-linked immunosorbent assay for therapeutic drug monitoring of cetuximab, Ther. Drug Monit. 31 (2009) 597–601.

[27] D.A. Blake, R.M. Jones, R.C. Blake, A.R. Pavlov, I.A. Darwish, H. Yu, Antibody-based sensors for heavy metal ions, Biosens. Bioelectron. 16 (2001) 799–809.

[28] L. Campanella, E. Martini, M. Tomassetti, Further development of lactoferrin immunosensor (part III), J. Pharm. Biomed. Anal. 53 (2010) 186–193.

[29] C. Tlili, L.N. Cella, N.V. Myung, V. Shetty, A. Mulchandani, Single-walled carbon nanotube chemoresistive label-free immunosensor for salivary stress biomarkers, Analyst 135 (2010) 2637–2642.

[30] L.M. Bonanno, T.C. Kwong, L.A. DeLouise, Label-free porous silicon immunosensor for broad detection of opiates in a blind clinical study and results comparison to commercial analytical chemistry techniques, Anal. Chem. 82 (2010) 9711–9718.

[31] A.W. Drake, D.G. Myszka, S.L. Klakamp, Characterizing high-affinity antigen/antibody complexes by kinetic- and equilibrium-based methods, Anal. Biochem. 328 (2004) 35–43.

[32] Y.W. Chiu, Q.X. Li, A.E. Karu, Selective binding of polychlorinated biphenyl congeners by a monoclonal antibody: analysis by kinetic exclusion fluorescence immunoassay, Anal. Chem. 73 (2001) 5477–5484.

[33] L. Xie, R.M. Jones, T.R. Glass, R. Navoa, Y. Wang, M.J. Grace, Measurement of the functional affinity constant of a monoclonal antibody for cell surface receptors using kinetic exclusion fluorescence immunoassay, J. Immunol. Meth. 304 (2005) 1–14.

[34] I.A. Darwish, T.A. Wani, N.Y. Khalil, D.A. Blake, Novel automated flow-based immunosensor for measurement of the breast cancer CA15-3 in serum, Talanta 97 (2012) 499–504.

[35] I.A. Darwish, T.A. Wani, N.Y. Khalil, Development of automated flow immunosensor based on kinetic exclusion analysis for measurement of α-fetoprotein in serum, Dig. J. Nanomater. Biostruct. 7 (2012) 493–500.

[36] I.A. Darwish, A.M. Alanazi, T.A. Wani, N.Y. Khalil, M.A. Hamidaddin, Novel automated flow-based immunosensor for real-time measurement of the breast cancer prognostic marker 2`-deoxycytidine in plasma, Dig. J. Nanomater. Biostruct. 8 (2013) 69–79.

[37] Y. Zhou, A.L. AL Goenaga , B.D. Harms, H. Zou, J. Lou, F. Conrad, G.P. Adams, B. Schoeberl, U.B. Nielsen, J.D. Marks, Impact of intrinsic affinity on functional binding and biological activity of EGFR antibodies, Mol. Cancer Ther. 11 (2012) 1467–76.

[38] A.G. Pallis, L. Serfass, R. Dziadziusko, J.P. van Meerbeeck, D. Fennell, D. Lacombe, J. Welch, C. Gridelli, Targeted therapies in the treatment of advanced/metastatic NSCLC, Eur. J. Cancer 45 (2009) 2473–2487.

[39] Genentech, Inc, About Avastin: proposed mechanism of action, 2017. https://www.avastin-hcp.com/about-avastin/proposed-moa.html.

[40] A. Sandler, R. Gray, M.C. Perry, J. Brahmer, J.H. Schiller, A. Dowlati, R. Lilenbaum, D.H. Johnson, Paclitaxel-carboplatin alone or with bevacizumab for non-small-cell lung cancer, N. Engl. J. Med. 355 (2006) 2542–2550.

[41] J. Mendelsohn, The epidermal growth factor receptor as a target for cancer therapy, Endocr. Relat. Cancer 8 (2001) 3–9.

[42] P.M. Fracasso, H. Burris, M.A. Arquette, R. Govindan, F. Gao, L.P. Wright, S.A. Goodner, F.A. Greco, S.F. Jones, N. Willcut, C. Chodkiewicz, A. Pathak, G.M. Springett, G.R. Simon, D.M. Sullivan, R. Marcelpoil, S.D. Mayfield, D. Mauro, C.R. Garrett, A phase 1 escalating single-dose and weekly fixed-dose study of cetuximab: pharmacokinetic and pharmacodynamic rationale for dosing, Clin. Cancer Res. 13 (2007) 986–993.

[43] P.J. Carter, L.G. Presta, Humanized antibodies and methods for making them, U.S. Patent No 6,054,297, Genentech, Inc., South San Francisco, Calif, 2000.

[44] GaBi online, Building trust in cost-effective treatments, Generics and Biosimilars Initiative, 2017. http://gabionline.net/Biosimilars/General/Biosimilars-of-cetuximab.

[45] L. Rios, A.A. Garcia, Dendrimer based non-competitive fluoroimmunoassay for analysis of cortisol, React. Funct. Polym. 68 (2008) 307–314.

[46] I. Hemmil, Fluoroimmunoassays and immunofluorometric assays, Clin. Chem. 31 (1985) 359–370.

[47] Sapidyne Instruments Inc, KinExA Technology operation manual, draft 1.0.8.0 direct to systems using software version 2.0.1.26, Boise, ID, USA, 2010.

[48] B.E. Kaplan, L.J. Hefta, K.M. Swiderek, J.E. Shively, Solid phase synthesis and characterization of carcinoembryonic antigen (CEA) domains, J. Pept. Res. 52 (1998) 249–260.

[49] I.A. Darwish, T.A. Wani, A.M. Alanazi, M.A. Hamidaddin, S. Zargar, Kinetic-exclusion analysis-based immunosensors versus enzyme-linked immunosorbent assays for measurement of cancer markers in biological specimens, Talanta 111 (2013) 13–19.

[50] T.A. Wani, I.A. Darwish, An automated flow immunosensor based on kinetic exclusion analysis for measurement of a free β-subunit of human chorionic gonadotropin in serum, New J. Chem. 36 (2012) 1114–1120.

[51] T.A. Wani, S. Zargar, S. Majid, I.A. Darwish, Analytical application of flow immunosensor in detection of thyroxine and triiodothyronine in serum, Assay Drug Dev. Technol. 14 (2016) 535–542.

[52] T.A. Wani, S. Zargar, S.M. Wakil, I.A. Darwish, New analytical application of antibody-based biosensor in estimation of thyroid-stimulating hormone in serum, Bioanalysis 8 (2016) 625–632.

[53] J.A. Thompson, F. Grunert, W. Zimmermann, Carcinoembryonic antigen gene family: molecular biology and clinical perspectives, J. Clin. Lab. Anal. 5 (1991) 344–366.

[54] ICH, Validation of analytical procedures: text and methodology, London, 2005.

[55] J.L. Bender, P.C. Adamson, J.M. Reid, L. Xu, S. Baruchel, Y. Shaked, R.S. Kerbel, E.M. Cooney-Qualter, D. Stempak, H.X. Chen, M.D. Nelson, M.D. Krailo, A.M. Ingle, S.M. Blaney, J.J. Kandel, D.J. Yamashiro, Phase I trial and pharmacokinetic study of bevacizumab in pediatric patients with refractory solid tumors: a children's oncology group study, J. Clin. Oncol. 26 (2008) 399–405.

[56] J.W.A. Findlay, W.C. Smith, J.W. Lee, G.D. Nordblom, I. Das, B.S. DeSilva, M.N. Khan, R.R. Bowsher, Validation of immunoassays for bioanalysis: a pharmaceutical industry perspective, J. Pharm. Biomed. Anal. 21 (2000) 1249–1273.

[57] T.J. McFarland, A.D. Rhoads, M. Hartzell, G.G. Emerson, A.R. Bhavsar, J.T. Stout, Bevacizumab levels in breast milk after long-term intravitreal injections, Retina 35 (2015) 1670-1673.

[58] N. Grebenchtchikov, A.J. Geurts-Moespot, L. Heijmen, H.W. van Laarhoven, C.M. van Herpen, A.M. Thijs, P.N. Span, F.C. Sweep, Quantification of patient-specific assay

interference in different formats of enzyme-linked immunoassays for therapeutic monoclonal antibodies, Ther. Drug Monit. 36 (2014) 765-770.

[59] J. Hantash, M. Smidt, R.R. Bowsher, The development, optimization and validation of an ELISA bioanalytical method for the determination of cetuximab in human serum, Anal. Methods 1 (2009) 144-148.

[60] C. Delbaldo, J.Y. Pierga, V. Dieras, S. Faivre, V. Laurence, J.C. Vedovato, M. Bonnay, M. Mueser, A. Nolting, A. Kovar, E. Raymond, Pharmacokinetic profile of cetuximab (Erbitux) alone and in combination with irinotecan in patients with advanced EGFR-positive adenocarcinoma, Eur. J. Cancer 41 (2005) 1739-1745.

[61] I.A. Darwish, M.M. Al-Shehri, M.A. El-Gendy, Development of new ELISA with high sensitivity and selectivity for bioanalysis of bevacizumab: a monoclonal antibody used for cancer immunotherapy, Curr. Anal. Chem. 14 (2018) 174-181.

[62] M.M. Al-Shehri, M.A. El-Gendy, I.A. Darwish, Development of specific new ELISA for bioanalysis of cetuximab: a monoclonal antibody used for cancer immunotherapy, Curr. Pharm. Anal. 14 (2018) 519-525.

Figure legends

Figure 1. Schematic representation of the operation of the KinExA system (A) and principles of flow fluorescent noncompetitive assay for mAbs: BEV and CET (B). Antigens coated on PMMA beads are VEGF and EGFR for the assay of BEV and CET, respectively. Fluorescence of FITC-IgG is continuously monitored during flow by a photodiode array detector facing the flow cell of the instrument and the signals are recorded via a PC interface.

Figure 2. KinExAgrams obtained by the KinExA^{TM} instrument for varying concentrations of BEV (left-hand panels: A,B) and CET (right-hand panels: C,D). Bottom panels (B,C) are the same signals of top-panels (A,C); however, they are presented on different scale of fluorescence (volts).

Figure 3. Titrations of antigens with corresponding antibodies. VEGF versus BEV (●) and EGFR versus CET (▼). Values are the mean of 3 determinations ± SD.

Figure 4. Effect of FITC-IgG concentration on the fluorescence signals for measurement of the immune complexes: VEGF-BEV (●, top axis) and EGFR-CET (▼, bottom axis) bound onto PMMA beads. Values are the mean of 3 determinations ± SD.

Figure 5. Calibration curves (●) and their precision profiles (▲) of the proposed KinExA-based assay for measurement of BEV (A) and CET (B).

Figure 6. KinExAgrams obtained for varying plasma dilutions containing BEV (15 ng mL^{-1}) and CET (400 ng mL^{-1}) . Panels A and B are for BEV and CET, respectively. Panel C represent the effect of plasma matrix on the analytical recovery on the assay of plasma-spiked BEV (●) and CET (▲); values are the mean of 3 determinations.

Figure 1

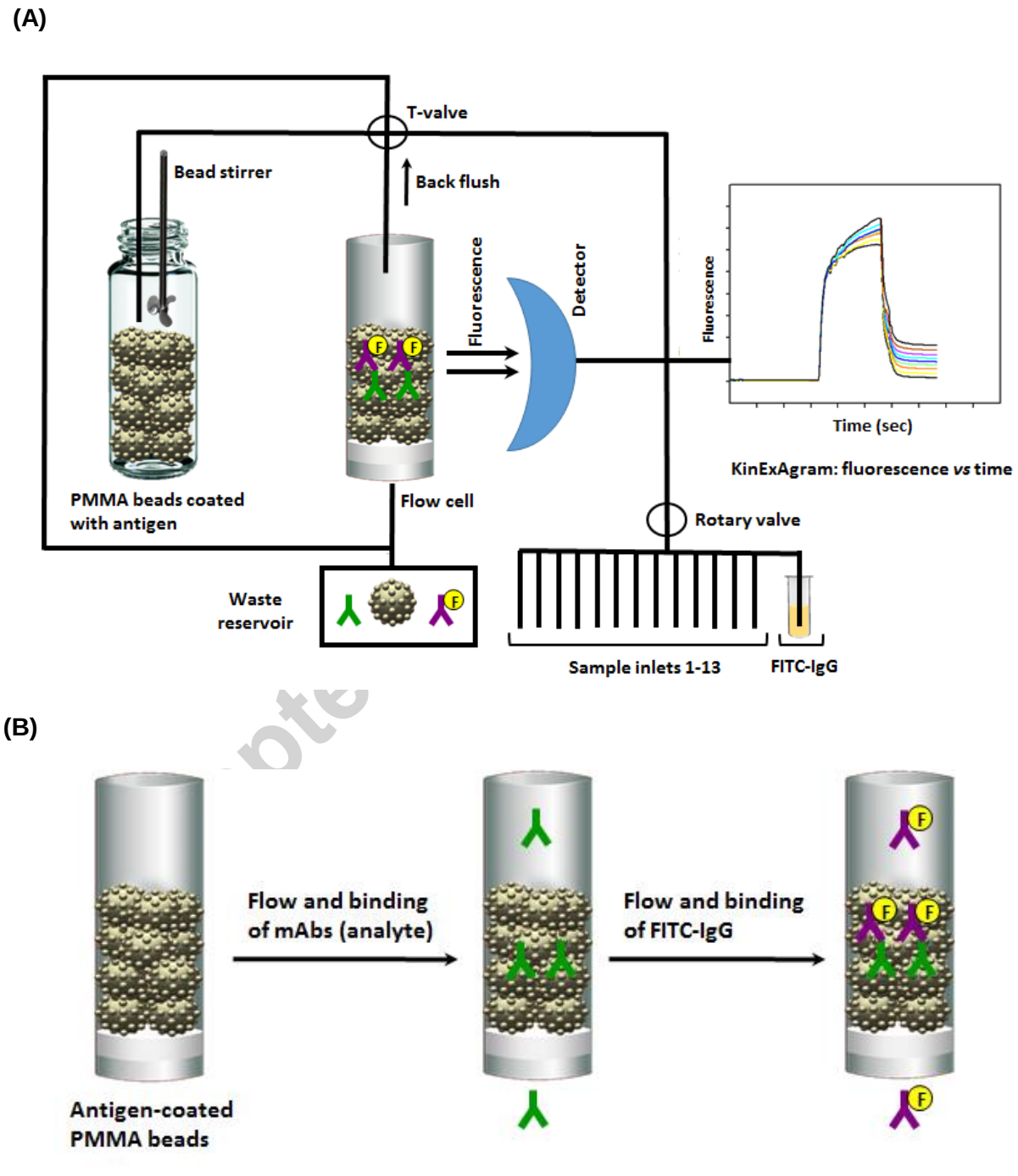
(A)
T-valve
Bead stirrer
Back flush
Fluorescence
Detector
Fluorescence
Time (sec)
KinExAgram: fluorescence vs time
PMMA beads coated with antigen
Flow cell
Rotary valve
Waste reservoir
Sample inlets 1-13
FITC-IgG
(B)
Flow and binding of mAbs (analyte)
Flow and binding of FITC-IgG
Antigen-coated PMMA beads

Figure 2

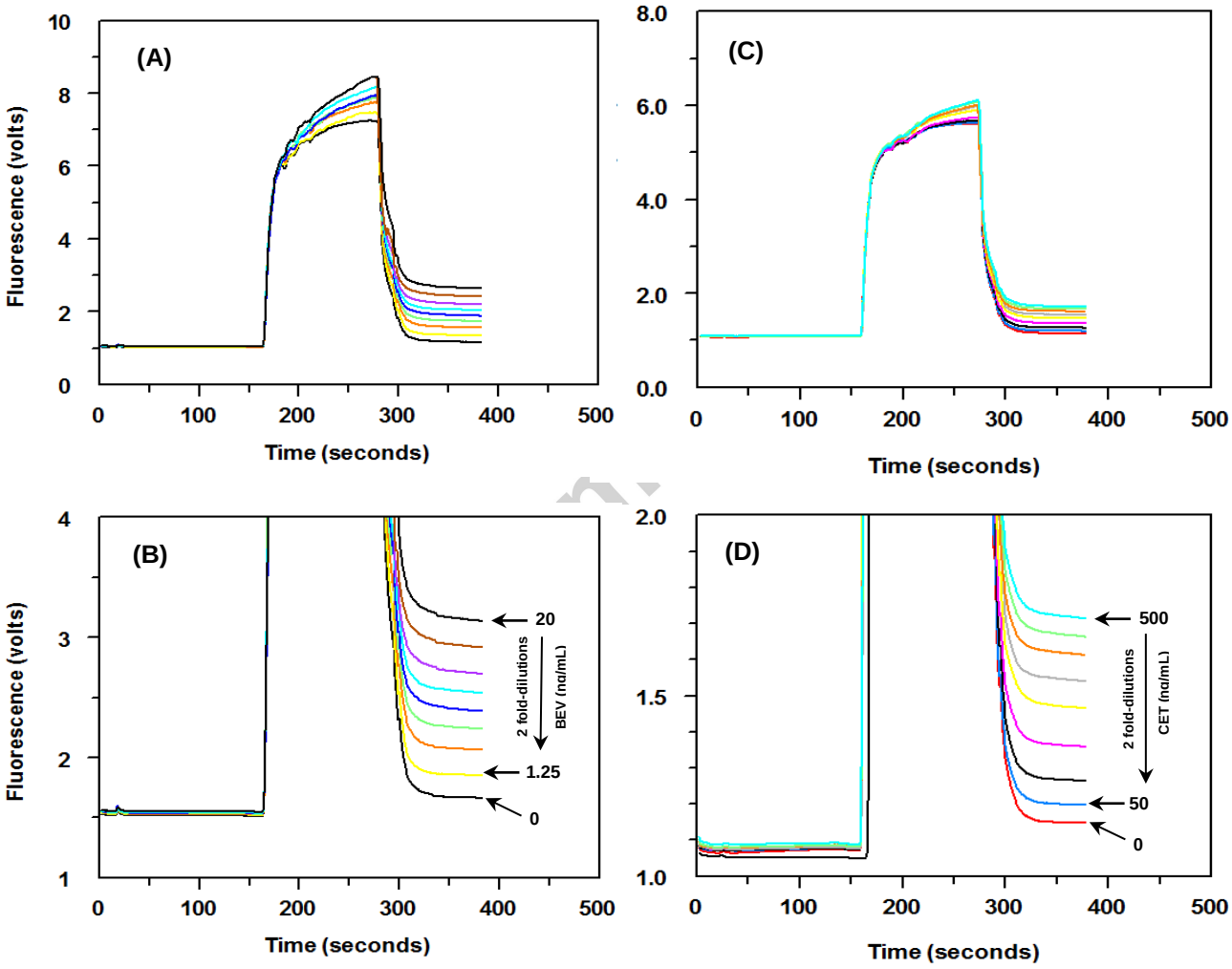

Figure 3

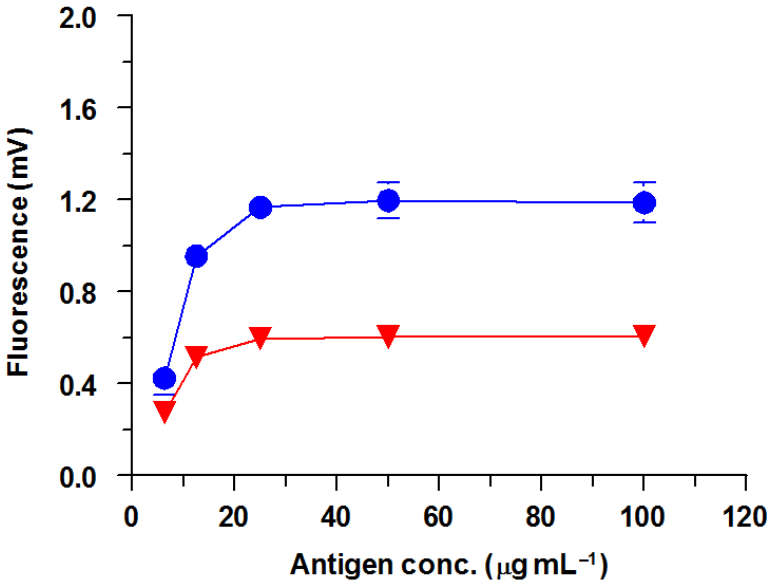

Figure 4

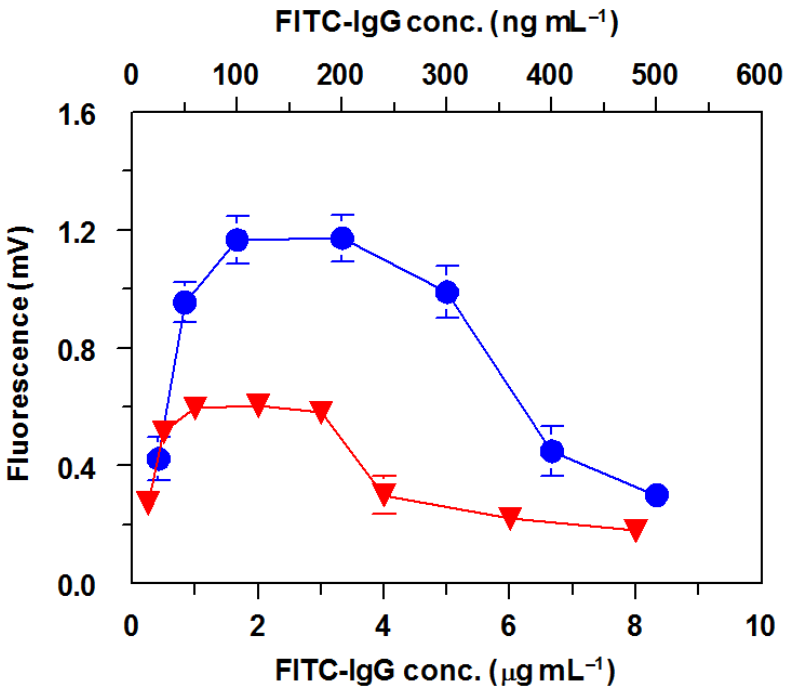

Figure 5

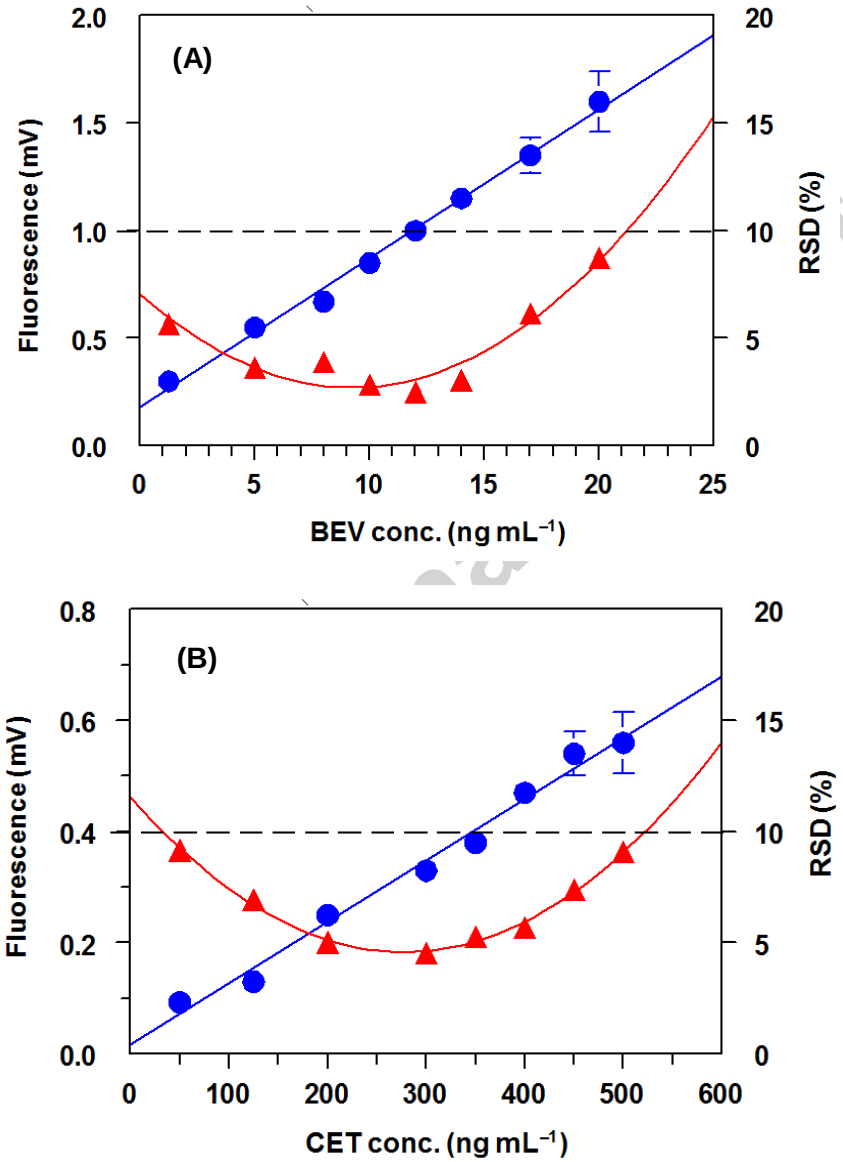

Figure 6

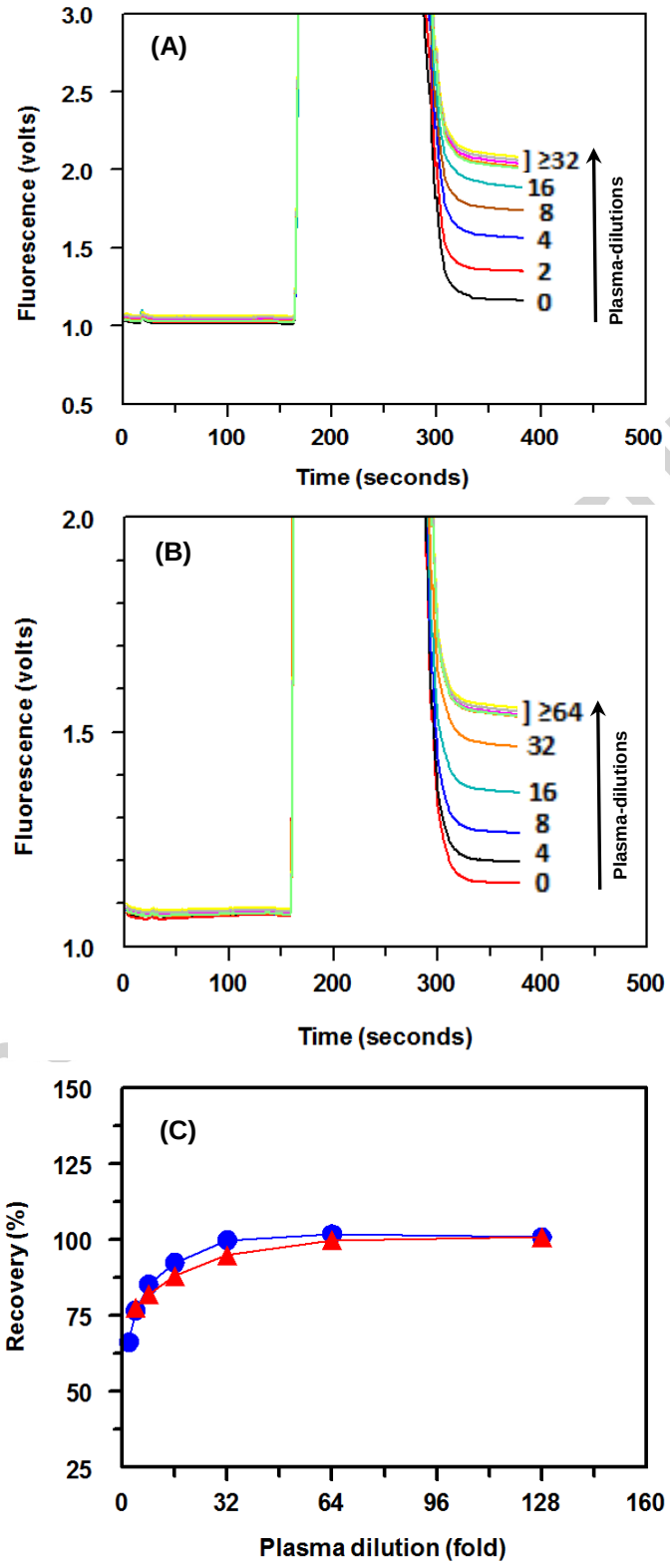

Table 1: Optimization of conditions for KinExA-based assay for BEV and CET

Condition	Optimum value	
	BEV	CET
Coating antigen (µg mL^{-1})	VEGF (50)	EGFR (50)
Volume of beads suspension (µL)	583	583
Flow rate of beads suspension (mL min^{-1})	1	1
Time of bead drawing (sec)	35	35
Secondary antibody (ng mL^{-1})	200	2
Volume of sample (µL)	500	500
Time of samples drawing (sec)	120	120
Volume of secondary antibody (µL)	500	500
Flow rate (mL min^{-1})	0.25	0.25

Table 2. Results of regression analysis for the calibration curves of KinExA for BEV and CET

Parameter	Value	
	BEV	CET
Linear dynamic range (ng mL^{-1})	1.25 – 20	50 – 500
Intercept	0.1782	0.0163
Slope	0.0693	0.0011
Determination coefficient (r^2)	0.994	0.987
LOD (ng mL^{-1})	1.28	52.64
LOQ (ng mL^{-1})	3.89	159.52

Table 3. Precision and accuracy of the proposed KinExA-based assay for BEV and CET

Intra-day precision			Inter-day precision		
Spiked conc. (ng mL^{-1})	Measured conc. (ng mL^{-1})	Recovery (% ± RSD)	Spiked conc. (ng mL^{-1})	Measured conc. (ng mL^{-1})	Recovery (% ± RSD)
		BEV			
2	2.1	102.5 ± 5.7	2	1.9	96.2 ± 4.8
4	4.1	103.2 ± 3.6	4	4.0	99.2 ± 2.7
8	7.9	98.6 ± 3.9	8	8.3	104.3 ± 4.2
16	16.2	101.4 ± 2.8	16	16.6	103.6 ± 2.2
	Mean	101.4 ± 4.0		Mean	100.8 ± 3.5
		CET			
100	99.2	99.2 ± 4.5	100	105.3	105.3 ± 5.2
200	193.6	96.8 ± 5.3	200	203.0	101.5 ± 6.1
300	306.3	102.1 ± 5.7	300	298.2	99.4 ± 2.5
400	390.0	97.5 ± 3.4	400	414.8	103.7 ± 3.7
	Mean	98.9 ± 4.7		Mean	102.5 ± 4.4

HIGHLIGHTS

- Automated flow fluorescent immunoassay was developed for bevacizumab (BEV) and cetuximab (CET).
- BEV and CET are monoclonal antibodies used for immunotherapy of cancers.
- The assay employed the noncompetitive binding format on the KinExA™ biosensor.
- The assay can accurately measure BEV and CET at concentrations as low as 3.9 and 159.5 ng mL^{-1}, respectively.
- The developed KinExA-based assay is superior to all the existing immunoassays.
- The assay has a great value in therapeutic monitoring of BEV and CET.